Fermi-LAT Observations of Extended Gamma-Ray Emission in the Direction of SNR G150.3+4.5

Jamie M. Cohen, Daniel Castro, Elizabeth Hays, John W. Hewitt

ABSTRACT

We report here a dedicated analysis of the γ-ray emission around supernova remnant (SNR) G150.3+4.5, observed with the Large Area Telescope (LAT) on board the *Fermi Gamma-Ray Space Telescope*. The Second Catalog of Hard *Fermi* LAT Sources reported detection of a hard spectrum, spatially extended source from 50 GeV - 2TeV, partially overlapping G150.3+4.5. Lowering the energy threshold to 1 GeV, we significantly detect a large ($\sigma = 1.40^\circ \pm 0.03^\circ$) extended γ-ray source consistent with the entirety of the radio shell and displaying a power law spectral index of 1.82 ± 0.04. An obtained HI spectrum toward the SNR suggests that the remnant could be one of the closest to us and estimates of its age indicate that G150.3+4.5 may be in the Sedov-Taylor phase [JAM: not sure about this, maybe distance is very uncertain, and hence age as well? My age estimate was $\sim$ 6kyr. Need to think about dynamically young vs. young, fast shocks like which SNR? does dynamically young say something more about the progenitor explosion or surrounding medium?]. In contrast, the spectrum of the γ-ray source is more akin to that of a young, leptonic dominated SNR, although ROSAT X-ray observations show no signs of nonthermal emission coincident typically observed in young SNRs. We discuss alternate origin scenarios for the γ-ray emission... [JAM: Should I have the words Pass 8 here somewhere, make it all shorter? move the on board stuff to intro.]

Subject headings: Supernova Remnants, γ-rays, Cosmic rays, Radio

1. Introduction

Supernova remnants have long been thought to be the primary accelerators of cosmic rays up to the knee of the cosmic ray energy spectrum.

what to say about radio SNRs? Connect CRs to nonthermal emission and the LAT and Something about SNRs, cosmic ray accelerators, radio detections, connection between radio-LAT observations, G150 detection, 2FHL blind detection and SNRs at TeV (all young?)

Focus more on the hadronic vs leptonic since that's what's interesting? We describe the LAT and analysis results in §2, detail multiwavelength observations in §3, and discuss various emission origin scenarios in §4.

2. *Fermi* LAT Observations and Analysis

2.1. Data Set and Reduction

Fermi LAT is a pair conversion telescope sensitive to high energy γ-rays from 20 MeV to greater than 1 TeV (Ackermann et al. 2016), operating primarily in a sky-survey mode which views the entire sky every 3 hours. The LAT has a wide field of view ($\sim$2.4 sr), a large effective area of $\sim$8200 cm^2 above 1 GeV for on axis events and a 68% containment radius angular resolution of $\sim 0.8^\circ$ at 1 GeV. For further details on the instrument and its performance see Atwood et al. (2009) and Ackermann et al. (2012).

In this analysis, we analyzed 7 years of Pass 8 data, from August 2nd 2008 to August 2nd 2015. The Pass 8 event reconstruction provides a significantly improved angular resolution [JAM: this is sadly unimportant unless I'm at higher energy or using the PSF types. The P8 total PSF at 1 GeV

is about the same as for P7REP. It's the acceptance/effective area that are considerably better at this energy], acceptance, and background event rejection (Atwood et al. 2013a,b), all of which lead to an increase in the effective energy range and sensitivity of the LAT. Source class events were analyzed within a 14°x14° region centered on SNR G150.3+4.5 using the P8R2_SOURCE_V6 instrument response functions, with a pixel size of 0.1°. To reduce contamination from earth limb γ-rays, only events with zenith angle less than 100° were included.

For spectral and spatial analysis we utilized both the standard *Fermi* Science Tools (version 10-01-01)[1] , and the binned maximum likelihood package `pointlike` (Kerr 2010). `pointlike` provides methods for simultaneously fitting the spectrum, position, and spatial extension of a source, and was extensively validated in Lande et al. (2012). Both packages fit a source model, the Galactic diffuse emission, and an isotropic component (which accounts for the background of misclassified charged particles and the extragalactic diffuse γ-ray background)[2] to the observations. In this analysis, we used the standard Galactic diffuse ring-hybrid model scaled for Pass 8 analysis, gll_iem_v06.fits (modulated by a power law function with free index and normalization), and for the isotropic emission, we used iso_P8R2_SOURCE_V6_v06.txt, extrapolated to 2 TeV as in Ackermann et al. (2016).

In our source model for the region, we included sources from the third *Fermi* LAT catalog (Acero et al. 2015, 3FGL) within 15° of the center of our region of interest (RoI). We replaced the position and spectrum of any 3FGL pulsars in the region with their corresponding counterpart from the LAT 2nd pulsar catalog (Abdo et al. 2013). Residual emission unaccounted for by 3FGL sources is present in the RoI due to the increased time range and different energy selection with respect to that in 3FGL. We added to the RoI several significant (TS $\geq$ 16) point sources to account for this unmodeled emission and minimize the global residuals. The closest of these sources added was about 1° away from the edge of the best fit GeV disk. [JAM: Considering the size of the PSF at 1 GeV, the affect of these sources on the disk fit was assumed to be negligible. do I need to say more about these sources? should I mention adding them automatically and iteratively based on TS maps and reference SNRcat/2FHL?]. The normalization and spectral index of sources within 5° of the center of the RoI were free to vary, whereas all other source parameters were fixed. A preliminary maximum likelihood fit of the RoI was performed, and sources with a test statistic (TS) < 9 (TS is defined as, TS $= 2$ Log$(\mathscr{L}_1/\mathscr{L}_0)$ where $\mathscr{L}_1$ is the likelihood of source plus background and $\mathscr{L}_0$ that of just the background) were removed from the model.

[1] `http://fermi.gsfc.nasa.gov/ssc/`

[2] `http://fermi.gsfc.nasa.gov/ssc/data/access/lat/BackgroundModels.html`

2.2. Morphological Analysis

Studying the spatial extension of sources with the LAT is non-trivial due to the energy-dependent point spread function (PSF) and strong diffuse emission present in the Galactic plane. Soft spectrum point sources and uncertainties in the diffuse model can act as sources of systematic error when not accurately modeling extended emission as such, particularly at low energies where the PSF is broad. To strike a balance between the best angular resolution and minimal source and diffuse contamination, we restrict our morphological analysis to energies between 1 GeV and 1 TeV. We divide this energy range into 12 [JAM: 4bpd] logarithmically spaced bins for both `pointlike` and `gtlike` binned likelihood analyses.

Three unidentified 3FGL sources are located within the extent of G150.3+4.5. 3FGL J0425.8+5600, located approximately 0.6° from the center of the SNR, is the closest of the three sources and is described with a power law spectrum of index $\Gamma = 2.35 \pm 0.17$ in the 3FGL catalog. The closest radio source to 3FGL J0425.8+5600 is NVSS J042719+560823, at 0.25 away (Ref?). 3FGL J0423.5+5442, exhibits a power law spectral index, $\Gamma = 2.63 \pm 0.15$, with no clear multiwavelength source association. Finally, 3FGL J0426.7+5437 has a pulsar-like spectrum, yet in a timing survey performed with the 100-m Effelsberg radio telescope, Barr et al. (2013) were unable to detect pulsations from the source down to a limiting flux density of $\sim$ 0.1 mJy. This source is located about 0.8° from the center of the SNR. We discuss 3FGL J0426.7+5437 and

potential association with G150.3+4.5 further in §4.2).

In our analysis, we removed 3FGL J0425.8+5600 and 3FGL J0423.5+544 from the RoI, but kept 3FGL J0426.7+5437 in the model since preliminary analyses showed clear positive residual emission at the position of the source if it was removed from the RoI. Figure 1 shows a residual TS map for the region around G150.3+4.5. This point source detection-significance map was created by placing a point source modeled with a power law of photon index $\Gamma = 2$ at each pixel and gives the significance of detecting a point source at each location above the background.

We modeled the excess emission in the direction of G150.3+4.5 with a uniform intensity, radially-symmetric disk, simultaneously fitting the spatial and spectral components of the model via `pointlike`. The extension of the disk was initialized with a seed radius of $\sigma = 0.1^\circ$ and position centered on the radio position of G150.3+4.5. We define the significance of extension as in Lande et al. (2012); $\mathrm{TS_{ext}} = 2\log(\mathscr{L}_{\mathrm{ext}}/\mathscr{L}_{\mathrm{ps}})$, with $\mathscr{L}_{ext}$ being the likelihood of the model with the extended source and $\mathscr{L}_{ps}$ that of a point source located at the peak of emission interior to the extended source. For the disk model we found that $\mathrm{TS_{ext}} = 298$, for the best fit radius, $\sigma = 1.40^\circ \pm 0.03^\circ$, and position, R.A. $= 55.46^\circ \pm 0.03^\circ$, DEC. $= 66.91^\circ \pm 0.03^\circ$, all in excellent agreement with the radio SNR size and centroid determined in Gao & Han (2014). [JAM: do other LAT papers give the TS of extended source too? TS = 373]. We tried adding back in to our model the two removed 3FGL sources but both were insignificant when fit on top of the best fit disk. The bottom map in Figure 1 is a residual TS map of the same region as the top map of the same Figure, but with the disk source included in the background model, demonstrating that the disk can account well for the emission in the region and justifying the exclusion of the two aforementioned 3FGL sources.

The morphology of the radio emission is suggestive of an elliptical or ring morphology, so both of these spatial models were tested as well. For the ring model, the fit reduced to a disk with parameters matching those stated above. Using the elliptical model showed a weak improvement over the radially symmetric model at the 2.6σ level

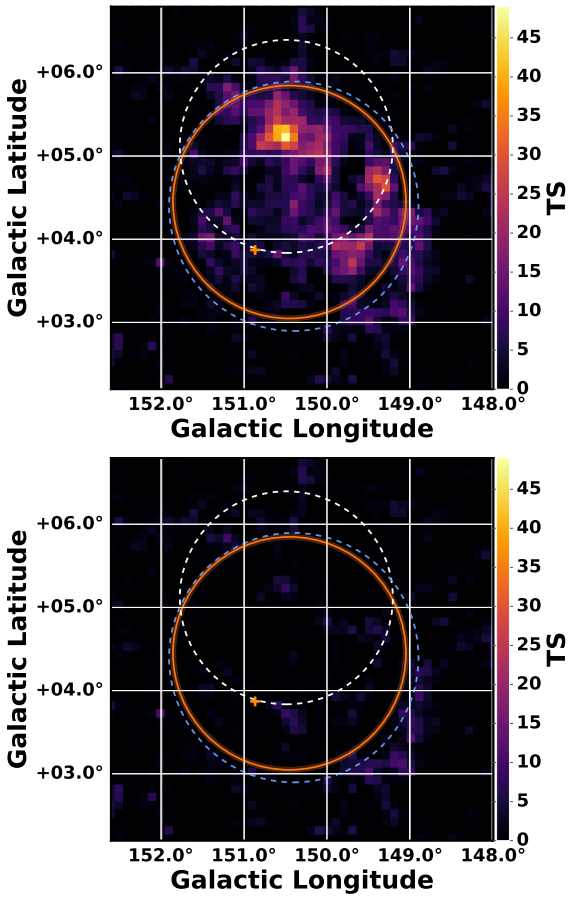

Fig. 1.— Background subtracted residual TS map above 1 GeV with 0.1°x 0.1° pixels, centered on SNR G150.3+4.5. The orange circle and translucent shading show the fit disk radius and 1σ errors, respectively, for the extended source, the orange cross shows the position of 3FGL J0426.7+5437 (included in the background model), blue dashed circle is the extent of the radio SNR, and white dashed circle depicts 2FHL J0431.2+5553e. Bottom map includes G150.3+4.5 in the background model, top does not.

(ΔTS = 9 with two additional degrees of freedom), which we did not consider significant enough to say the GeV emission had an elliptical morphology (see Table 1). For the remainder of this study, we only considered the disk spatial model. [JAM: double check this for 1GeV- 1TeV. I was done for 1-562 GeV, running it now!]

2FHL J0431.2+5553e is the extended source

detected in the 2FHL catalog found to be overlapping the northern region of G150.3+4.5 Ackermann et al. (2016). The source has a power law spectral index $\Gamma = 1.66 \pm 0.2$, and disk radius $\sigma = 1.27^\circ \pm 0.04^\circ$ (see Figure 1). When comparing the best fit extension of the 2FHL source with the result from this paper, factoring in the uncertainty in both extension and position, we see that the > 50 GeV and > 1 GeV results are not incompatible. It is likely that the paucity of events above 50 GeV is the cause of the smaller fit radius, as opposed to the difference arising from the effects of an energy dependent morphology. To explore the connection between the 2FHL and above 1 GeV emission, we tested a few other spatial hypotheses.

First, we replaced the $\sigma = 1.40^\circ$ disk with an another disk matching the spectral and spatial parameters of 2FHL J0431.2+5553e and calculated the likelihood with this new source's position and extension fixed. For this hypothesis, we find $\mathrm{TS_{ext}} = 165$, and $\mathrm{TS} = 226$, demonstrating that the fixed disk matching the 2FHL source is clearly disfavored over the previously determined best fit disk at this energy. Our next test consisted of placing a second extended source on top of the best fit disk detected above 1 GeV. We added a source, initially matching the spatial and spectral parameters of 2FHL J0431.2+5553e, to our source model of the region (in addition to the $\sigma = 1.40^\circ$ disk), and fit its spectrum and extension. Fitting a second extended source in this region serves two purposes: 1. it acts as a check on whether there was residual emission unaccounted for by the previously best-fit disk, and 2. it allows us to determine if the best fit disk can be split into two spectrally distinct, components. This fit resulted in the source wandering north (but still partially overlapping G150.3+4.5) and having an insignificant extension, $\mathrm{TS_{ext}} = 4$. Details on the spatial parameters are given in Table 1.

[JAM: Something about J0426?like how modeling G150 as point vs extended if it's really extended can affect the fit of other point sources nearby, like J0426, so show the spectrum of this source too? I fit both the norm and index of the source. Save this for discussion? How does the spectrum of J0426 change with the new source? Maybe the most that needs to be said is that below 1 GeV it's confused with]

[JAM: from Josh's paper: modelling the spectrum of an intrisically extended source as point sources skews the PS spectrum to softer energies "Specifically, modeling a spatially extended source as point-like will systematically soften measured spectra", idk if I get why. We see it with the 2 removed 3FGL sources being softer than what the disk winds up being.]

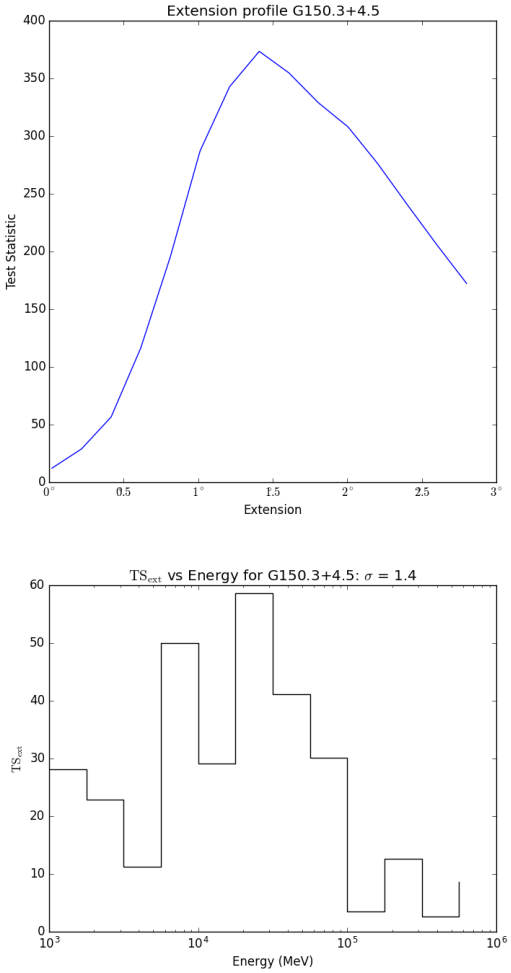

Fig. 2.— Not sure I want to include these, replot, get rid of titles, and make them look nicer if I do want to include. Top plot shows that the TS peaks at the best fit extension. Lower plot gives a sense of how significant the extension is (vs a point source) across the analyzed energy range. If I keep, add text in the section

TABLE 1
EXTENDED ANALYSIS RESULTS

Spatial Model	TS_{ext}	TS [a]	σ [°]	R.A. [°]	DEC [°]
Disk	278.843	-32.850	49.80	LMC	gal
Elliptical Disk	189.048	3.033	398.64	IC 443	snr
2FHL J0431.2+5553e (free spatial) [b]	260.317	-3.277	63.87	Puppis A	snr
2FHL J0431.2+5553e (fixed spatial)	260.317	-3.277	63.87	Puppis A	snr
Disk & 2FHL J0431.2+5553e [b]	260.317	-3.277	63.87	Puppis A	snr

NOTE.— Haven't filled in real numbers for G150 yet just copied from 2FHL table. Not sure I need this table yet? Other things to add N_{dof}, LL, spectral params?

[a]Calculated in `gtlike`

[b]Started with disk matching the spectral/spatial parameters of 2FHL J0431.2+5553e and fit them.

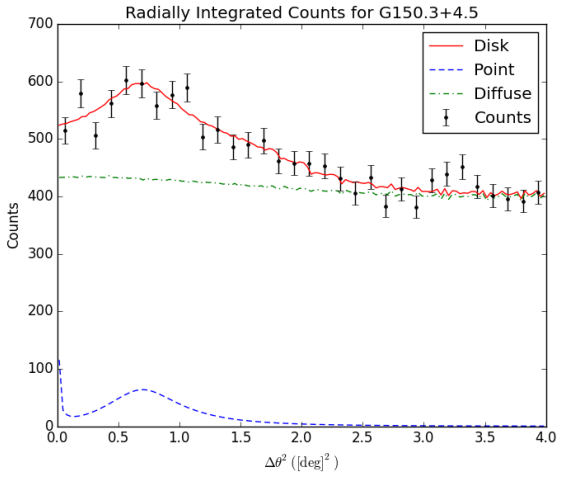

Fig. 3.— Include this to show that there's significant emission above the background? Replot without the point model.

2.3. Spectral Analysis

After determining the best fit morphology with `pointlike` for the GeV emission coincident with SNR G150.3+4.5, we used those results as a starting point for our `gtlike` maximum-likelihood fit of the region to estimate the best spectral parameters for our model. The LAT data is well described by a power law from 1 GeV to 1 TeV with a photon index, $\Gamma = 1.82 \pm 0.04$, and energy flux above 1 GeV of (7.17 ± 0.73) x10^{-11} erg cm^{-2} s^{-1}and TS = 389 [JAM: pointlike results were index = 1.80 flux = $(7.17 \pm 0.73$ x$10^{-11})$ erg cm^{-2} s^{-1}]. We tested the γ-ray spectrum of the extended disk for spectral curvature using a log-normal model (Log Parabola), and find no significant deviation from a power law (ΔTS $\sim$ 1). Figure 6 shows the best-fit power law spectral energy distribution for the GeV source whose morphology was described in Section 2.2. Spectral data points were obtained by dividing the energy range into 12 logarithmically spaced bins and modeling the source with a power law of fixed spectra index, $\Gamma = 2$.

[JAM: what else to include here? Systematics. Bracketing IRFs, alt iem, try varying the extension? still to be done.]

3. Multiwavelength Observations and Analysis

3.1. HI

3.2. CO?

Jack's looking into Planck data for HI and CO

3.3. X-ray

No diffuse nonthermal X-ray emission observed by ROSAT. No point sources near the center? Should a pulsar even be near the center? How to quantify this? Can we place a limit on ambient density with an upper limit on thermal X-ray emission? Magnetic filed with nonthermal?

4. Discussion and Results

4.1. What is it?

I haven't been calling the GeV source G150.3+4.5 this whole time. should I be?

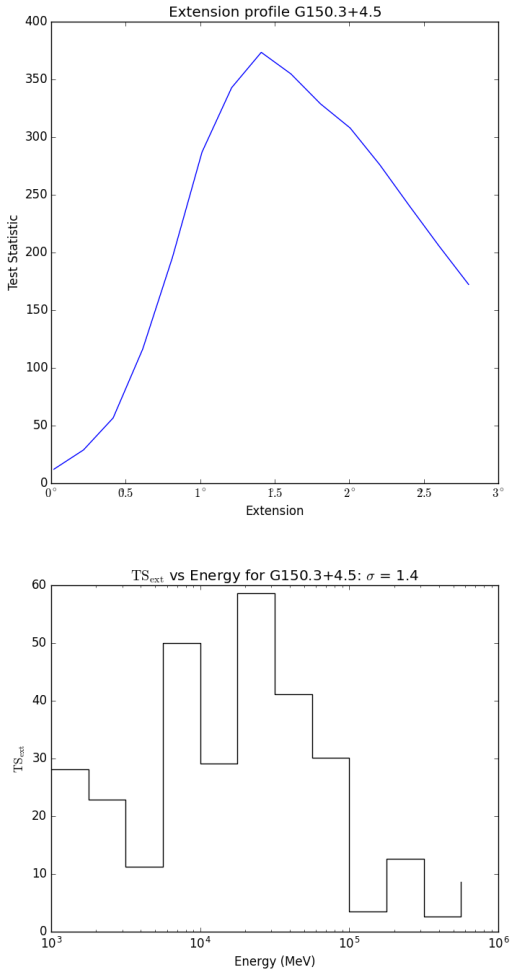

Fig. 4.— Not sure I want to include these, replot, get rid of titles, if I do want to include.

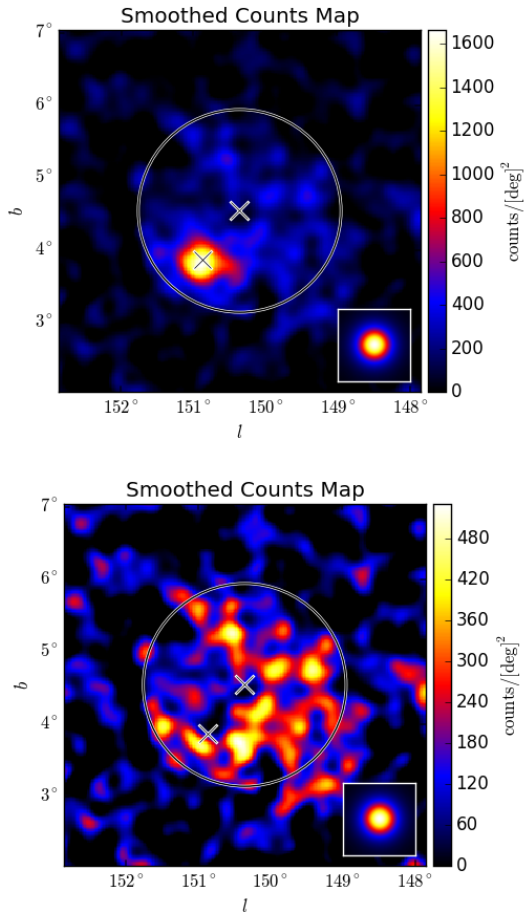

Fig. 5.— Should I include (diffuse subtracted) counts map of the region to show what the actual counts (not just TS map) like and where the 3FGL sources are? (redo these removing the extended source and including the 3FGL? or 3FGL removed in a diffetent color? Not sure I need these and the TS maps. Redo them as pdf/eps. Remove titles, use same cmap as figure 1, bigger bolder font.

Size + HI suggest that near distance corresponding to different HI velocities suggest it's aged, spectrum looks more like young SNR (hard + no GeV break). Is it a weird young remnant or weird aged one? Leptonic dominated if young, hadronic dominated if older? Something about nearby dense clouds masking hadronic emission? Maybe this is only true for MeV cosmic rays that are screened out though and it would only mask the pion bump, but not this higher energy emission?

PWN or SNR. Can we rule out PWN? See W41 paper, MSH 11-61A, Fabios recent G326 work (no, he just tries to use the PSF types and testing different model templates to try to disentangle SNR from PWN)?

No PSR candidate near center (should it be near the center? Depends on age) Is there some limit we can place on the PWN based on not seeing the pulsar? Like on Edot? OR something like Mattana et al. 2009 correlation between $\mathrm{flux_x}/\mathrm{flux_g} \propto$ Edot?

Assume it's in Sedov phase based on size + near

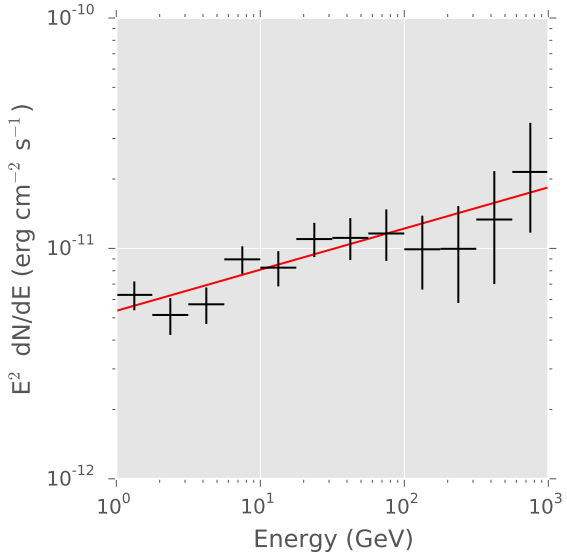

Fig. 6.— Spectral energy distribution for the extended source coincident with SNR G150.3+4.5 from 1 GeV to 1 TeV. Red line corresponds to the best fit power law model. Crosses are shown with with statistical error bars [JAM: add systematics when I have them]. [JAM: Butterfly?]

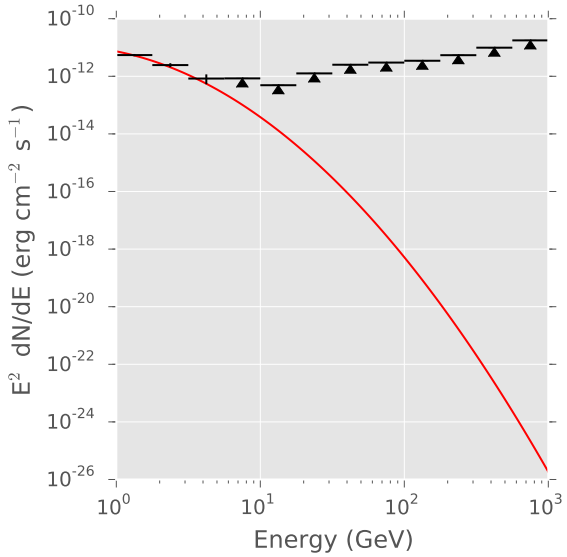

Fig. 7.— Spectral energy distribution of 3FGL J0426.7+5437. [JAM: Replot this make it look nicer]

distance, and calculate age, upper limit on Edot base on lack of x-ray flux? Or maybe if I assume the sources is the PWN and GeV radius is PWN radius, then can I estimate Edot based on size and evolution inside SNR?

If we assume close distance, age is only ≈ 5kyr, maybe this is a transitional SNR? What do others like this look like? Puppis A? Gamma Cygni is a similar age too.something

Say something about what the radio index is and the connection to the gev index [JAM: remake the G150 all SNR SEDs with the new gtlike data points]

4.2. Distance Considerations

probably doesn't need to be a different section.

4.3. Nonthermal Modeling

Have a working model using naiama. What more needs to be done?

Add bremss. properly scale the radio flux density. Talk to Dan about whether it makes sense. Are there params that I can fix? Kep, B? Any reason to have different n? Liz had doubts about the pp component extending to such high energy, is this really an issue?

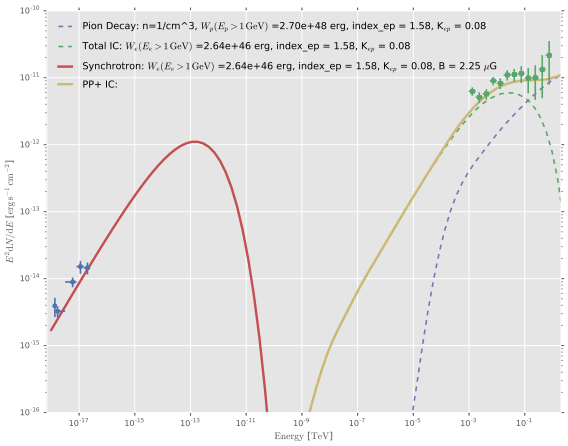

Fig. 8.— G150.3+4.5. Naima SED [JAM: bigger font, get rid of text for each line]

TABLE 2
NAIMA PARAMETERS

Spatial Model	TS_{ext}	TS ,[a]	σ [°]	R.A. [°]	DEC [°]
Disk	278.843	-32.850	49.80	LMC	gal
Elliptical Disk	189.048	3.033	398.64	IC 443	snr
Disk + 2FHL	260.317	-3.277	63.87	Puppis A	snr
2FHL (No Disk)	260.317	-3.277	63.87	Puppis A	snr

NOTE.— Add table with results from naima model? Two cols with param name and value? Split for fit and fixed params? These are just the same vals from table 1 for now

[a]Calculated in `gtlike`

5. Conclusions

REFERENCES

Abdo, A. A., et al. 2013, ApJS, 208, 17

Acero, F., et al. 2015, ArXiv:1501.02003

Ackermann, M., et al. 2012, ApJS, 203, 4

—. 2016, ApJS, 222, 5

Atwood, W., et al. 2013a, ArXiv:1303.3514

Atwood, W. B., et al. 2009, ApJ, 697, 1071

—. 2013b, ApJ, 774, 76

Barr, E. D., et al. 2013, MNRAS, 429, 1633

Gao, X. Y., & Han, J. L. 2014, A&A, 567, A59

Kerr, M. 2010, PhD thesis, University of Washington, arXiv:1101.6072

Lande, J., et al. 2012, ApJ, 756, 5

This 2-column preprint was prepared with the AAS LaTeX macros v5.2.